A Comparison of Isotropic (*MAT_224) and Anisotropic (*MAT_264) Material Models in High Velocity Ballistic Impact Simulations

Sean Haight [1], Paul Du Bois [2], and Cing-Dao "Steve" Kan [1]

[1] *Center for Collision Safety and Analysis (CCSA), George Mason University*
[2] *Consulting Engineer, Northville, MI*

Abstract

*To improve the modeling of metals in high velocity impacts, there have been many developments in constitutive material modeling for LS-DYNA®. One such advancement is the development of the Tabulated Johnson-Cook material model (*MAT_224). *MAT_224 is a tabulated material model with strain rate and temperature dependency. Additionally, this model includes a failure criteria as a function of triaxiality, Lode parameter, temperature, strain rate and element size. This model has been used successfully in the simulation of numerous materials in high velocity ballistic impact load cases.*

*One drawback to the original Tabulated Johnson-Cook material model is that it is implemented with von Mises isotropic plasticity. Therefore, this material model is not ideal for simulating metals that are anisotropic or asymmetric. Subsequently, an anisotropic and asymmetric version of the Tabulated Johnson-Cook model was developed to simulate these materials. The *MAT_264 material model maintains all the capabilities of the *MAT_224 model, but it adds the ability to define the material response in the 0-degree, 45-degree, 90-degree and thickness directions. Additionally, it allows for directional tension-compression asymmetry in the material. Strain rate dependency, temperature dependency, and the failure model are retained from the Tabulated Johnson-Cook model.*

*By using a previously developed failure model and limited material specimen testing, an industrial material characterization was developed for a 6.35 mm thick Ti-6Al-4V rolled plate. Specimen testing of this titanium alloy plate reveals that this material exhibits some anisotropy and asymmetry. NASA cylindrical ballistic tests were simulated with both the *MAT_224 and *MAT_264 material models. First, the isotropic implementation of the *MAT_264 material model is compared to the *MAT_224 model. Second, the anisotropic implementation of the *MAT_264 model is compared to the isotropic *MAT_224 model. Multiple impact velocities are simulated and the resulting exit velocities, internal energies and eroded internal energies are used to compare each material model.*

Introduction

Since its development in 2010, the Tabulated Johnson-Cook material model (*MAT_224) has been used to characterize metals in high velocity impact ballistic impact simulations [1] [2]. This constitutive model is designed to describe the material response of metals that can be affected by large deformations, high strain rates and thermal softening. The implementation of this model is based on tabulated inputs where the effective stress vs. effective plastic strain, or yield curve, is

provided by the user as functions of strain rate and temperature. In addition to the tabulated plasticity inputs, the Tabulated Johnson-Cook model also includes a failure criteria as a function of triaxiality, Lode parameter, temperature, strain rate, and element size. While this material model is very useful in characterizing isotropic metals in dynamic simulations, it does not have the ability to characterize anisotropic or orthotropic materials.

In 2016, an anisotropic and asymmetric version of the Tabulated Johnson-Cook model (*MAT_264) was developed to simulate the material response of anisotropic, or more specifically, orthotropic and asymmetric materials under dynamic loading [3] [4]. This material model was developed with a similar approach as the traditional Tabulated Johnson-Cook model, but allowed for tabulated inputs in the 0-degree, 45-degree, 90-degree and thickness directions. This was accomplished by introducing a new yield surface based on a combination of the Hill yield function and two orthotropic Lode parameters as proposed by Cazacu and Barlat [5]. This material was verified and validated for single elements, tension specimens and compression specimens.

One important characteristic of the orthotropic plasticity variant of the Tabulated Johnson-Cook model is that it is entirely backwards compatible with the traditional version. In other words, the anisotropic model should be able to reproduce the same results as the isotropic model if only 0-degree inputs are used for all directions.

The purpose of this research is to compare and contrast the results of these two material models in the simulation of high velocity ballistic impact tests performed by The National Aeronautics and Space Administration (NASA) [6]. First, the backwards compatibility of the anisotropic (*MAT_264) model to the isotropic (*MAT_224) model is tested. Second, the results from the anisotropic and asymmetric simulation of two projectile velocities will be compared to the results when the isotropic model (*MAT_224) is used.

Methodology

A set of simulations are designed to replicate a series of ballistic impact tests performed by the NASA at the Glenn Research Center [6]. These tests consist of a 381 mm by 381 mm Ti-6Al-4V plate with a thickness of 6.35 mm. These Ti-6Al-4V plates are mounted to a frame that has an inner diameter of 254 mm. A cylindrical projectile is manufactured with a diameter of 12.7 mm and a length of 22.225 mm. These projectiles were manufactured from an A2 tool steel material. This projectile is shot into the center of the plate from a gas gun at velocities ranging from 189 m/s to 278 m/s. Several high speed cameras were positioned around the area of impact to measure the velocity of the projectile prior to impact. If the projectile penetrated the plate specimen, then the exit velocity was also measured using a similar camera system.

The plate and projectile are modeled with solid elements with a mesh size of 0.2 mm (around the impact area). The projectile consists of 106,480 solid elements. The plate is modeled with 944,944 solid elements. The outer boundary condition is modeled as a perfectly rigid and fixed edge. Since the test report describes the projectiles as having no "evidence of plasticity or macro deformation", the A2 tool steel was modeled as an elastic element with no plastic deformation. This projectile is positioned so that it is pointed at the center of the specimen plate and normal to the surface of the plate. The initial velocity of the projectile is set based on the impact velocity described in the test report.
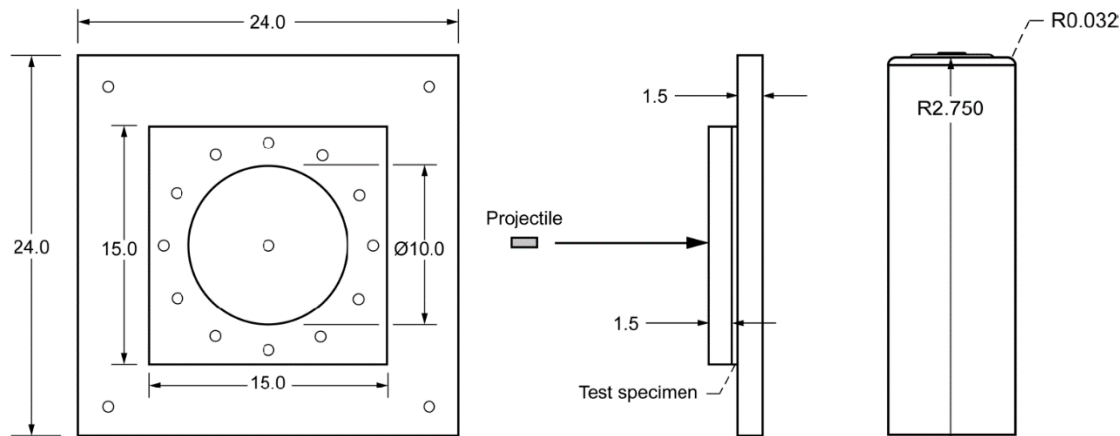
Figure 1: Ti-6Al-4V ballistic impact test setup [6]

To simulate the Ti-6Al-4V material with *MAT_224 (isotropic) and *MAT_264 (isotropic), a set of yield curves must be generated. The process for generating the yield curves from material test data is described in previous work by Haight et al. [2]. To characterize the material in *MAT_224, 2 tables (strain rate and temperature) are used to define the plasticity model and 4 tables/curves are used to describe the failure model. For *MAT_264, 18 tables (strain rate and temperature for each material direction) are used to define the plasticity and 4 tables/curves are used to define the failure model.

At the time of this writing, a limited material testing data set exists for this 6.35 mm thick Ti-6Al-4V plate [7]. High strain rate and high temperature tests have not been conducted for the 45-degree, 90-degree and thickness directions. Therefore, for the purposes of this comparative study, the strain rate and temperature effects will be estimated for all directions based on the strain rate and temperature effects found in a similar 12.7 mm thick Ti-6Al-4V plate [2]. A scale factor can be determined for the additional strain rates and temperatures. These scale factors are applied to the quasi-static and room temperature input yield curves for each material direction. For example, to determine the input yield curve for the 45-degree direction at a strain rate of 1.0E-3 /ms for the 6.35 mm plate: the 0-degree input yield curve at 1.0E-3 /ms that was determined for the 12.7 mm plate is first divided by the 0-degree input yield curve at the quasi-static strain rate for the same 12.7 mm plate. Then, the average value (as a function of plastic strain) of that resulting division operation is then multiplied by the 45-degree quasi-static (6.35 mm plate) input yield curve (at all values of plastic strain) resulting in the 45-degree 1.0E-03 /ms yield curve for the 6.35 mm plate. This procedure can be duplicated for all available strain rates and temperatures. This operation not only means that there is a single scale factor for each strain rate and temperature curve, but those scale factors are adapted from another Ti-6Al-4V plate.

Table 1 shows the scale factor for each strain rate (1/ms) in each material direction. The green scale factors are curves that have been generated directly from test data. The red scale factors have been estimated from the strain rate effects seen in a similar 12.7 mm thick Ti-6Al-4V plate [2]. Table 2 shows the scale factor for each temperature (K) in each material direction (0-degree Tension, 0-degree Compression, 45-degree Tension, etc.). Figure 2 shows the quasi-static and room temperature yield curves for each material direction. These yield curves are generated directly from the testing of this 6.35 mm Ti-6Al-4V plate.

Rate	Table #	QS	0.01	0.10	1.50	2.50	5.00	10.0	15.0	20.0	30.0	40.0	50.0
00T	100	1.0	1.007	1.032	1.086	1.105	1.135	1.189	1.417	1.87	2.32	2.79	3.24
00C	300	1.0	1.007	1.032	1.086	1.105	1.135	1.189	1.417	1.87	2.32	2.79	3.24
45T	800	1.0	1.007	1.032	1.086	1.105	1.135	1.189	1.417	1.87	2.32	2.79	3.24
45C	1100	1.0	1.007	1.032	1.086	1.105	1.135	1.189	1.417	1.87	2.32	2.79	3.24
90T	700	1.0	1.007	1.032	1.086	1.105	1.135	1.189	1.417	1.87	2.32	2.79	3.24
90C	1000	1.0	1.007	1.032	1.086	1.105	1.135	1.189	1.417	1.87	2.32	2.79	3.24
ThT	900	1.0	1.007	1.032	1.086	1.105	1.135	1.189	1.417	1.87	2.32	2.79	3.24
ThC	1200	1.0	1.007	1.032	1.086	1.105	1.135	1.189	1.417	1.87	2.32	2.79	3.24

Table 1: Strain rate (1/ms) input yield curve scale factors

Temp	Table #	RT	473	673	873
00T	200	1.0	0.727	0.553	0.461
00C	400	1.0	0.727	0.553	0.461
45T	1400	1.0	0.727	0.553	0.461
45C	1700	1.0	0.727	0.553	0.461
90T	1300	1.0	0.727	0.553	0.461
90C	1600	1.0	0.727	0.553	0.461
ThT	1500	1.0	0.727	0.553	0.461
ThC	1800	1.0	0.727	0.553	0.461

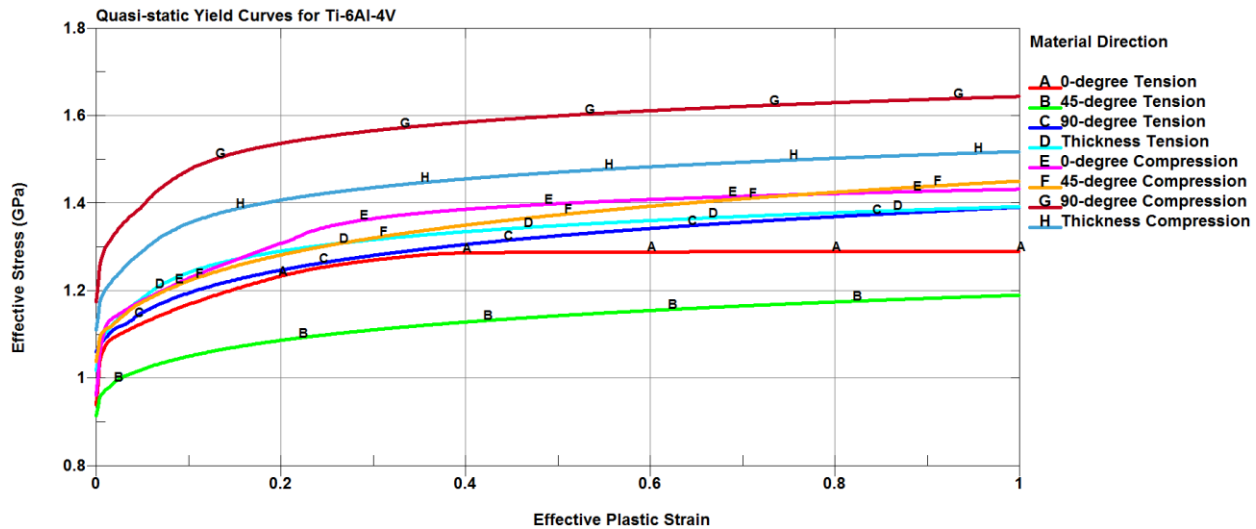*Table 2: Temperature (K) input yield curve scale factors*

Figure 2: Quasi-static and room temperature yield curves for each material direction
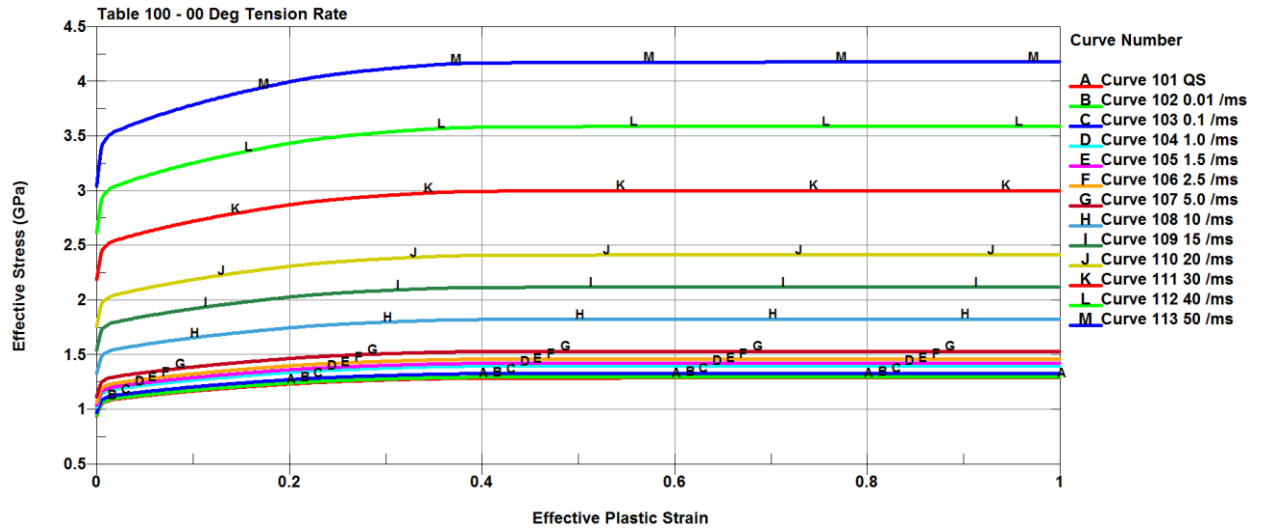
Figure 3: Example strain rate input table (0-degree tension) after quasi-static yield curve scaling

The full anisotropic material input for the Ti-6Al-4V plate is shown in Figure 4. Tables 100, 300, 500, 700, 800, 900, 1000, 1100 and 1200 are the strain rate dependent yield curve tables for 0-degree tension, 0-degree compression, 45-degree shear, 90-degree tension, 45-degree tension, thickness tension, 90-degree compression, 45-degree compression and thickness compression. Tables 200, 400, 600, 1300, 1400, 1500, 1600, 1700 and 1800 are the temperature dependent yield curve tables for the 0-degree tension, 0-degree compression, 45-degree shear, 90-degree tension, 45-degree tension, thickness tension, 90-degree compression, 45-degree compression and thickness compression. Additionally, the failure model is adapted from previous research with a similar Ti-6Al-4V plate [2]. This failure model is based on a surface which is a function of triaxiality and Lode parameters (table 3000). Additionally, the effect of strain rate (table 4000) and temperature (table 5000) are also incorporated into the failure model. Lastly, this model includes mesh regularization for failure (table 6000). The development of this failure model is described in a Federal Aviation Administration report [2]. No changes or alterations are made to this failure model, even though it was developed for a different titanium plate.

```
*MAT_TABULATED_JOHNSON_COOK_ORTHO_PLASTICITY
$      MID        RO         E        PR        CP        TR      BETA    NUMINT
         1 4.4300E-6 100.00000  0.342000 526.30000 293.00000  0.800000  1.000000
$     T00R      T00T       LCF       LCG       LCH       LCI
       100       200      3000      4000      5000      6000
$     C00R      C00T      S45R      S45T                SFIEPM     NITER      AOPT
       300       400       500       600                   2.5       100         2
$     T90R      T45R      TTHR      C90R      C45R      CTHR
       700       800       900      1000      1100      1200
$     T90T      T45T      TTHT      C90T      C45T      CTHT                   TOL
      1300      1400      1500      1600      1700      1800               0.001
$       XP        YP        ZP        A1        A2        A3      MACF
                                     1.0       0.0       0.0
$       V1        V2        V3        D1        D2        D3      BETA
                                     0.0       1.0       0.0
```

Figure 4: Anisotropic material input card for Ti-6Al-4V ballistic simulation

Figure 5 is the isotropic/symmetric material input card which will be used to compare to the isotropic Tabulated Johnson-Cook material model directly. This implementation uses the 0-degree tension rate and temperature input yield curves along with the previously described failure model. The shear yield is adapted to correspond to the values predicted by the von Mises criterion. The input card for the *MAT_224 material model is identical to the first two lines of Figure 5.

```
*MAT_TABULATED_JOHNSON_COOK_ORTHO_PLASTICITY
$      MID        RO         E        PR        CP        TR      BETA    NUMINT
         1 4.4300E-6 100.00000  0.342000 526.30000 293.00000  0.800000  1.000000
$     T00R      T00T       LCF       LCG       LCH       LCI
       100       200      3000      4000      5000      6000
$     C00R      C00T      S45R      S45T              SFIEPM     NITER      AOPT
       100       200       300       400                   2.5       100         2
$     T90R      T45R      TTHR      C90R      C45R      CTHR
       100       100       100       100       100       100
$     T90T      T45T      TTHT      C90T      C45T      CTHT                   TOL
       200       200       200       200       200       200               0.001
$       XP        YP        ZP        A1        A2        A3      MACF
                                      1.0       0.0       0.0
$       V1        V2        V3        D1        D2        D3      BETA
                                      0.0       1.0       0.0
```

Figure 5: Isotropic material input card for Ti-6Al-4V ballistic simulation (to test backward compatibility)

Results

The first series of ballistic simulations is to verify that the isotropic/symmetric implementation of the anisotropic model compares to the original (isotropic) tabulated Johnson-Cook material model. To accomplish this comparison, all of the anisotropic inputs for material model were based on the 0-degree tension input tables. Therefore, only the 0-degree tension (with strain rate and temperature dependency) were used in both the anisotropic model and the original tabulated Johnson-Cook model. The simulations were initialized with initial projectile velocities of 229 m/s and 278 m/s.

For each simulation, the internal energy and the eroded element internal energy was compared. Additionally, the velocity of the projectile as a function of simulation time was also compared for each material model. The contour of plastic strain at a specific simulation time was also compared for each model.

Figure 6 and Figure 7 show the internal and eroded internal energies for the 229 m/s and 278 m/s impacts. It is clear from these results that the isotropic implementation of the anisotropic *MAT_264 model is has equivalent energies to the original isotropic Tabulated Johnson-Cook model. Figure 8 shows the projectile velocities for each simulation as a function of simulation time. Figure 9 shows a section view of the plastic strain contour at a simulation time of 0.1 ms. The *MAT_224 (left) and isotropic *MAT_264 (right) simulations seem to have similar plastic strains for both impact velocities.
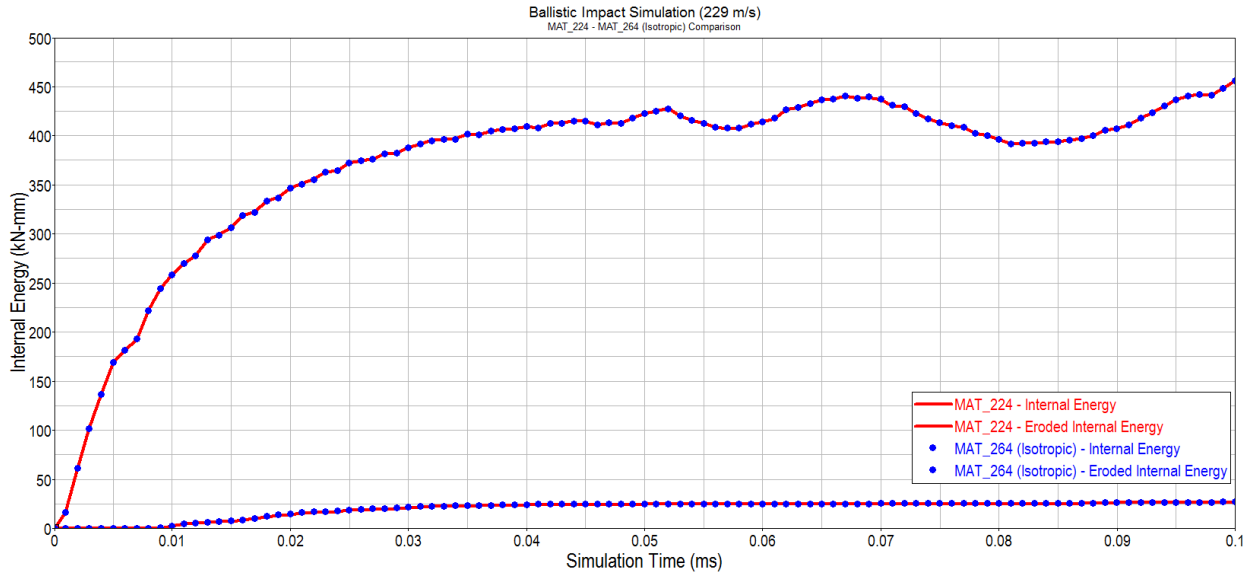
Figure 6: Internal Energy and Eroded Internal Energy for 229 m/s impact (isotropic *MAT_264 vs *MAT_224)
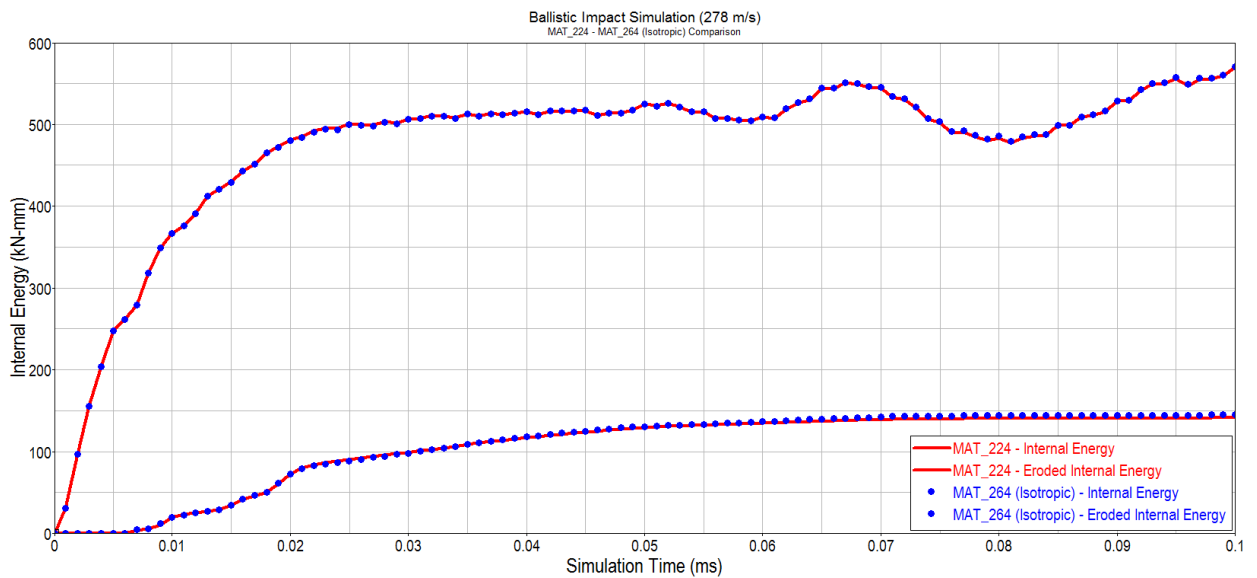

Figure 7: Internal Energy and Eroded Internal Energy for 278 m/s impact (isotropic *MAT_264 vs *MAT_224)
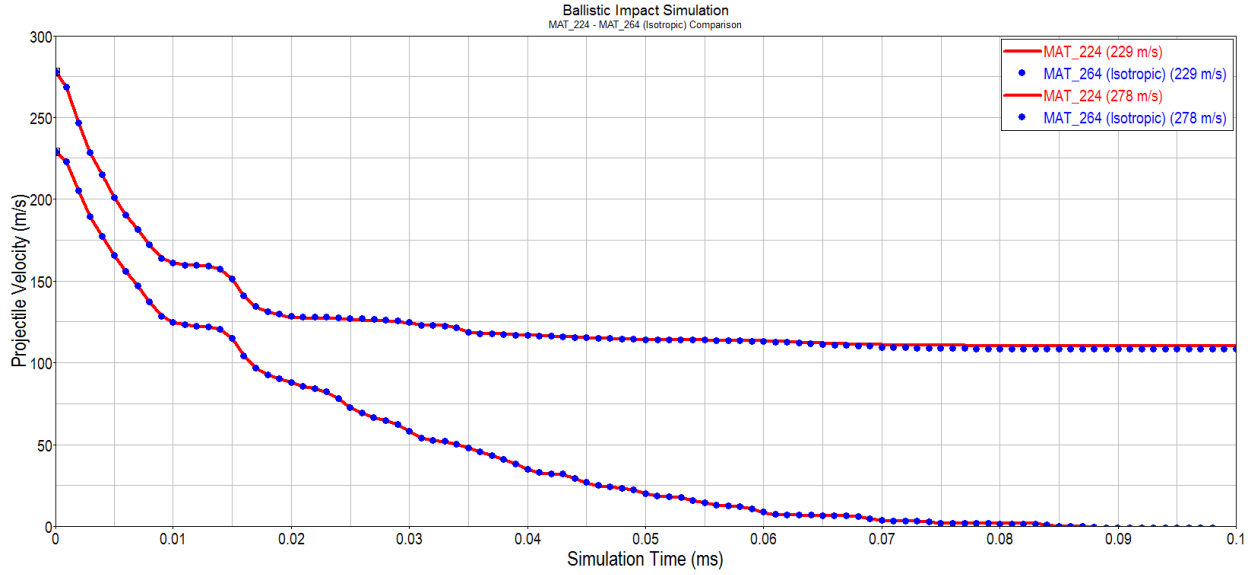
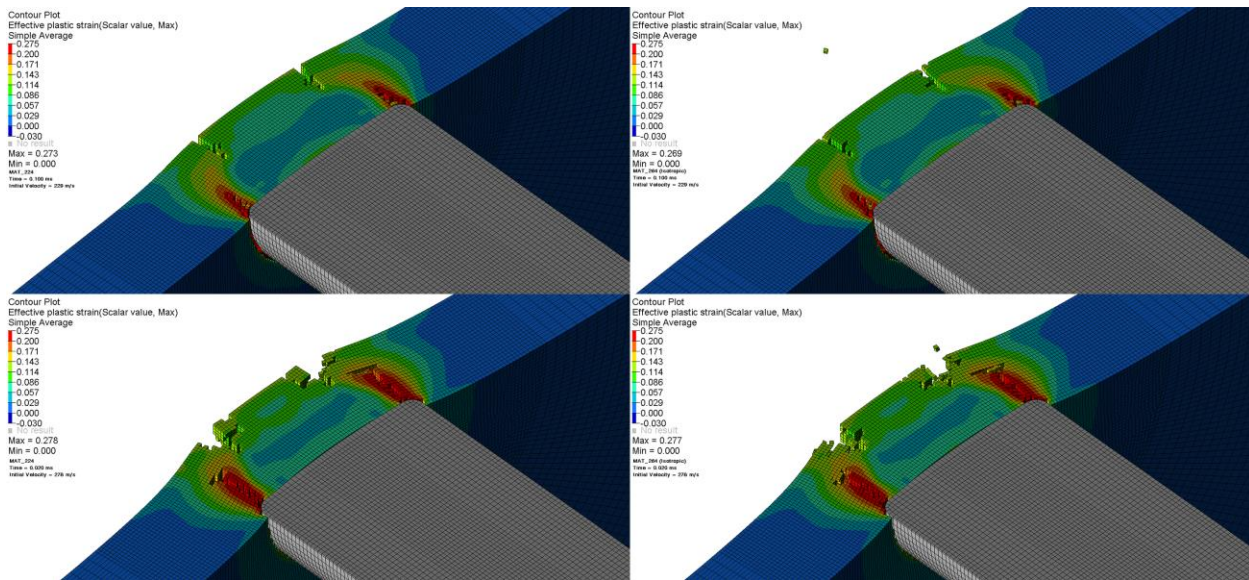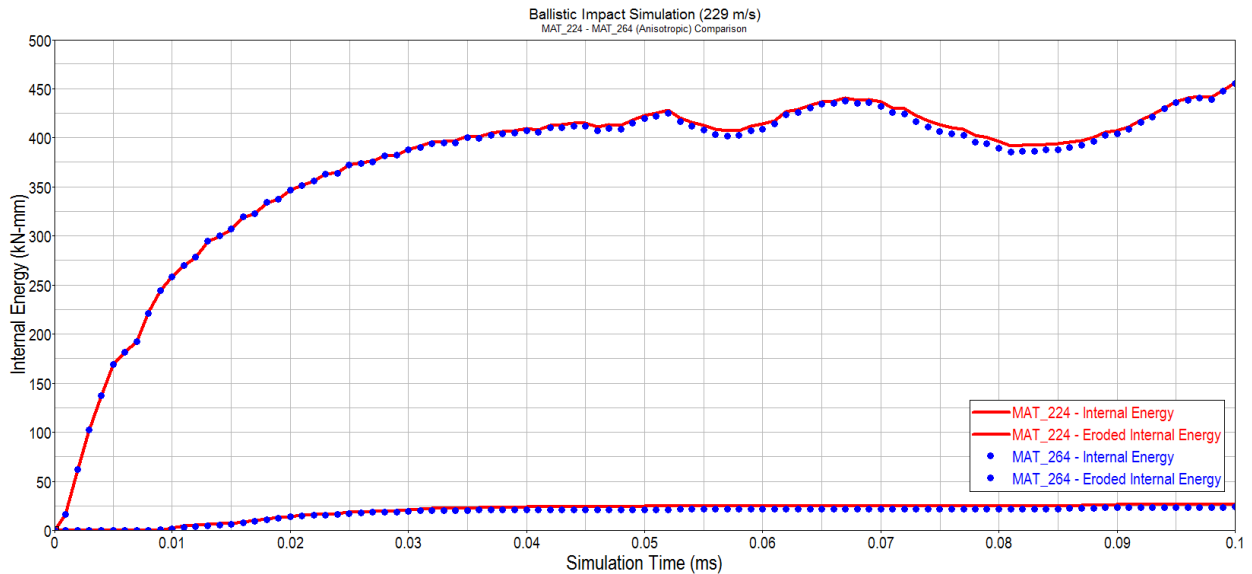***Figure 8: Projectile velocities for 229 m/s and 278 m/s impacts (isotropic *MAT_264 vs *MAT_224)***

Figure 9: Plastic strain contour for: *MAT_224 229 m/s (top left), isotropic *MAT_264 229 m/s (top right), *MAT_224 278 ms/s (bottom left) and isotropic *MAT_264 278 m/s (bottom right)

The second series of simulations is to compare a fully populated version of the anisotropic *MAT_264 to the isotropic *MAT_224. For this implementation of *MAT_264, all 18 tables of the material model were used as described in the methodology portion of this paper. For the *MAT_224 model, only the 0-degree tension (rate and temperature) tables and the failure model were used. The simulations were initialized with initial projectile velocities of 229 m/s and 278 m/s.

Figure 10 and Figure 11 show the internal and eroded internal energies for the 229 m/s and 278 m/s impacts. It is clear from these results that the anisotropic *MAT_264 model has different reported energies when compared to the isotropic *MAT_224 model. This difference is more pronounced at the larger impact velocity. Figure 12 shows the projectile velocities for each simulation as a function of simulation time. Figure 13 shows a section view of the plastic strain contour at a simulation time of 0.1 ms. The *MAT_224 (left) and isotropic *MAT_264 (right) simulations seem to have similar plastic strains for both impact velocities.

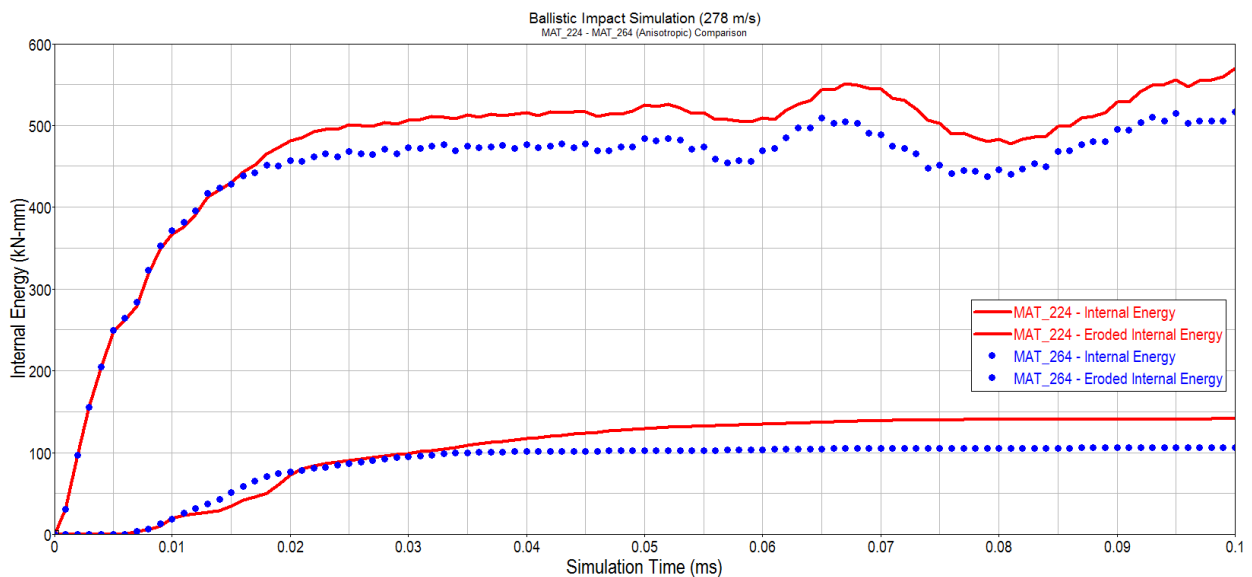*Figure 10: Internal Energy and Eroded Internal Energy for 229 m/s impact (*MAT_264 vs *MAT_224)*

*Figure 11: Internal Energy and Eroded Internal Energy for 278 m/s impact (*MAT_264 vs *MAT_224)*
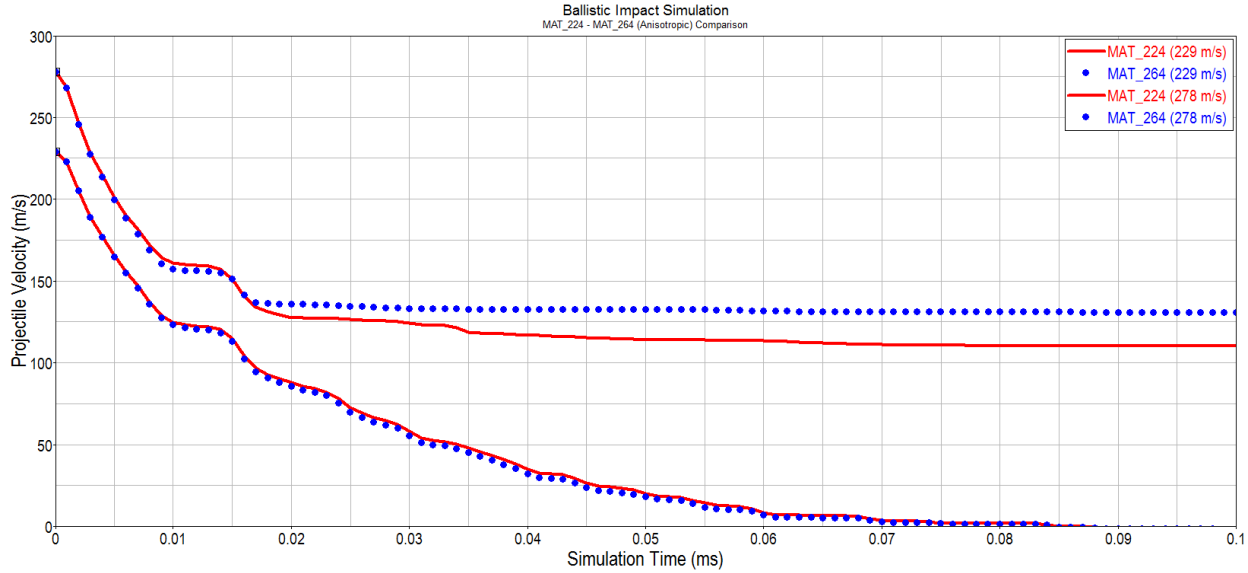
Figure 12: Projectile velocities for 229 m/s and 278 m/s impacts (*MAT_264 vs *MAT_224)
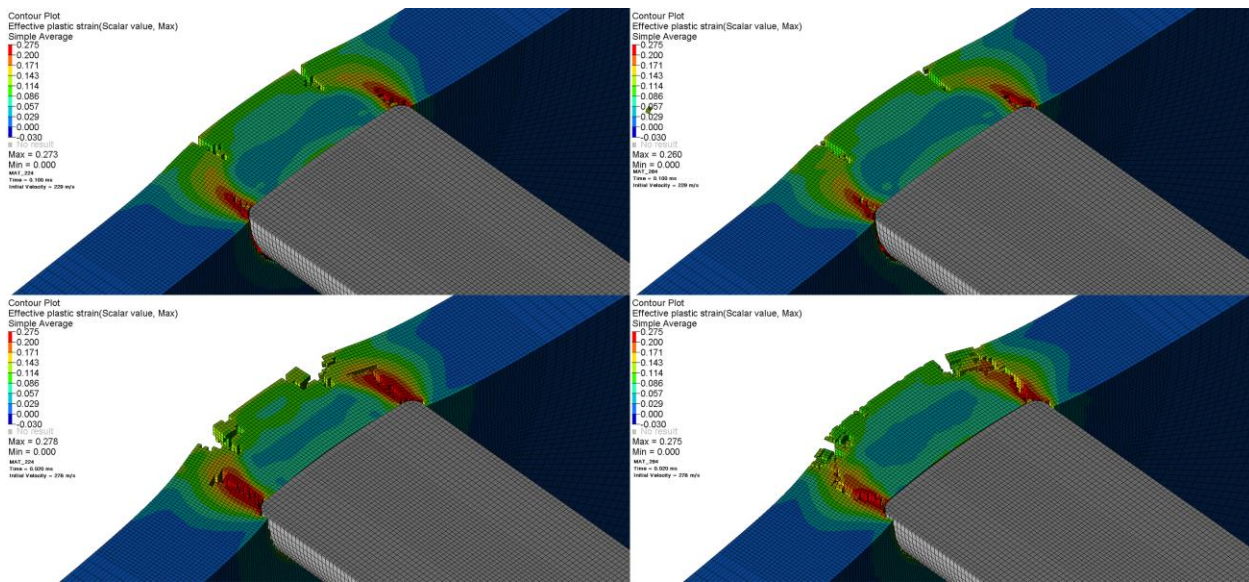

Figure 13: Plastic strain contour for: *MAT_224 229 m/s (top left), *MAT_264 229 m/s (top right), *MAT_224 278 ms/s (bottom left) and *MAT_264 278 m/s (bottom right)

Figure 14 shows an example of the von Mises stress contour for both the *MAT_224 (isotropic) and *MAT_264 (anisotropic) models. It is clear that yield stress directionality is evident in the anisotropic *MAT_264 model. As seen in Figure 2, the 0-degree and 90-degree yield stresses are similar while the 45-degree yield stress is considerably lower. This is consistent with the stresses shown in the contour plot using *MAT_264.
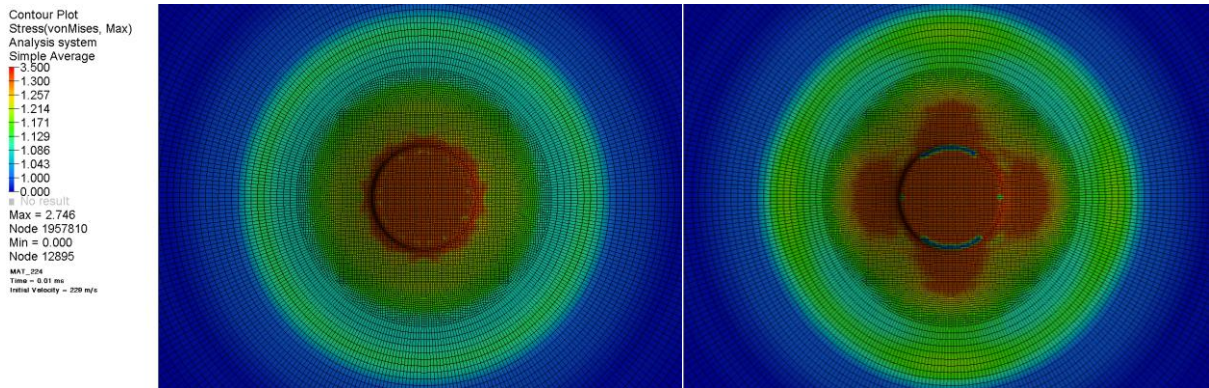
Figure 14: Von Mises Stress contour for *MAT_224 (left) and *MAT_264 (right)

Summary and Conclusions

The first objective of this study was to test the backwards compatibility of the recently developed Tabulated Johnson-Cook Ortho-Plasticity model (*MAT_264) relative to the original Tabulated Johnson-Cook model (*MAT_224). It was found that when only the 0-degree input data was used with *MAT_264, the internal energies, eroded internal energies and the plastic strain were consistent with the *MAT_224 result. In other words, the isotropic implementation of the anisotropic *MAT_264 model has similar results when compared to the isotropic *MAT_224 model. This is important because this model was based on the original *MAT_224 framework and was designed to be backwards compatible with previously developed tabulated Johnson-Cook models.

The second objective of this study was to examine the effects of using a fully populated *MAT_264 material card when compared to the *MAT_224 model. It was expected that there would be some difference between the results due to the influence of anisotropy and asymmetry in this Ti-6Al-4V plate. There was visible difference in the results between two models for simulations where the projectile was contained by the specimen plate, but the difference was more apparent when the projectile had some residual velocity. In total, the resulting energies, velocities and plastic strains are different when using the anisotropic *MAT_264 model. Lastly, the von Mises stress contours were compared to visualize the effect of the anisotropy. It was shown that the directionality of the yield stress does have an effect in the resulting stress contours. It was also clear that the relative yield stresses determined from the material specimen testing for each direction do correspond to the stress contours shown in the plate.

Since the material testing data was not available to completely populate the strain rate and thermal options of the *MAT_264 model, some of the input yield curves were estimated from the effects seen in a similar Ti-6Al-4V plate. Therefore, this study is limited to a general comparison of the two models, rather than a full validation of the materials ballistic limit or residual velocities. Future work can be conducted by expanding the material specimen testing to fully populate the material model. Additional directional strain rate and thermal testing can used to develop a full material characterization of this Ti-6Al-4V plate. Then, additional analysis can be completed to investigate the material models ability to predict the materials ballistic limit and residual velocities.

References

[1] M. Buyuk, "Development of a Tabulated Thermo-Viscoplastic Material Model with Regularized Failure for Dynamic Ductile Failure Prediction of Structures Under Impact Loading," United States Department of Transportation, Washington, DC, 2014.

[2] S. Haight, L. Wang, P. Du Bois, K. Carney and C.-D. Kan, "Development of a Titanium Alloy Ti-6Al-4V Material Model Used in LS-DYNA," United States Department of Transportation, Washington, DC, 2016.

[3] S. Haight, C.-D. Kan and P. Du Bois, "Development of a Fully-Tabulated, Anisotropic and Asymmetric Material Model for LS-DYNA (*MAT_264)," in *10th European LS-DYNA Conference*, Wurzburg, Germany, 2015.

[4] S. Haight, *Developement of a Fully-Tabulated, Anisotropic and Asymmetric Material Model for Simulation of Metals Under Dynamic Loading,* Fairfax, VA: George Mason University, 2016.

[5] O. Cazacu and F. Barlat, "A criterion for description of anisotropy and yield differential effects in pressure-insensitive metals," *Journal of International Plasticity,* vol. 20, pp. 2027-2045, 2004.

[6] J. M. Pereira, D. M. Revilock, B. A. Lerch and C. R. Ruggeri, "Impact Testing of Aluminum 2024 and Titanium 6Al-4V for Material Model Development," U.S. National Aeronautics and Space Administraion / U.S. Department of Transportation (FAA), Cleveland, OH, 2013.

[7] J. T. Hammer, *Plastic Deformation and Ductile Fracture of Ti-6Al-4V under Various Loading Conditions,* Columbus, OH: The Ohio State University, 2014.

Acknowledgments